NANO LETTERS

2007
Vol. 7, No. 10
3007−3012

Local Surface Charges Direct the Deposition of Carbon Nanotubes and Fullerenes into Nanoscale Patterns

Livia Seemann, Andreas Stemmer, and Nicola Naujoks*

Nanotechnology Group, ETH Zurich, Tannenstrasse 3, CH-8092 Zurich, Switzerland

Received June 5, 2007; Revised Manuscript Received July 25, 2007

ABSTRACT

This article reports on the directed deposition of carbon nanotubes (CNTs) and fullerenes onto solid surfaces using local electrostatic fields. Arbitrary patterns of local surface charges are created by charge writing with an atomic force microscope. During the subsequent development of the sample in an aqueous suspension containing surfactant-stabilized CNTs or fullerenes, Coulomb attraction guides the positioning and alignment of these particles onto the charge patterns. The surface potential of the charge patterns provides a direct control over the particle attachment. CNTs and fullerenes precisely reproduce the charge patterns, yielding structures with a lateral resolution down to the particle diameter.

Carbon nanotubes are known to have considerable potential as key components in future nanotechnological devices, such as field-effect transistors,[1] nanoscale actuators,[2] memory elements,[3] and sensors measuring chemical[4] or physical[5] quantities. However, to integrate individual carbon nanotubes into devices, it is crucial to have concepts for their precise placement and alignment. Current approaches include catalyst-pattern-directed growth,[6] electric-field-induced alignment,[7,8] flow cell methods,[9] and alignment based on self-assembled monolayers.[10] Likewise to carbon nanotubes, the spatially controlled deposition of C_{60} molecules onto surfaces still represents a challenging issue. The assembly of one-dimensional nanorods of fullerenes from solution on silicon[11] and the directed patterning of C_{60} by covalent attachment to chemically functionalized self-assembled monolayers[12] belong to the most recent approaches.

The controlled assembly of nanoscale objects into predefined structures, as well as their precise positioning, has been assessed by a variety of methods. Electrostatic fields have proven useful to guide the assembly process, and one example of employing electrostatic fields to precisely direct nanoparticles to desired locations on the sample surface is a method referred to as nanoxerography. Here, the electrostatic fields are created by local electric charges on the sample surface which, in a subsequent step, act as templates for the precise deposition of nanoscale objects. The charge patterns may be created by a stamping-like process, employing hard[13] or soft[14] micropatterned electrodes, or with the help of scanning-probe-based methods.[15] Deposition may be carried out either from the gas phase, as has been demonstrated by Jacobs et al.,[14] or from the liquid phase. For the deposition of particles from liquids, water-in-oil emulsions have been used to a large extent, including the assembly of silica microspheres,[15] gold colloids,[16] layered biomolecular structures,[17] and peptide fibrils.[18] Since the resolution is limited by the emulsion droplet size, smaller structures can only be fabricated when depositing the particles directly from suspension. This way, polymer beads[19] and multiwalled carbon nanotubes[20] have been deposited from alcohol-based suspensions.

Here we present the selective deposition of single-walled carbon nanotubes (SWCNTs) and C_{60} molecules from commonly used surfactant-based aqueous suspensions. Coulomb attraction guides the charged particles onto the previously charged locations. Both carbon nanotubes and C_{60} molecules reproduce the charge patterns with high precision leading to structures with excellent pattern definition. We show that the magnitude of the local surface potential strongly influences the deposition behavior, offering control over pattern resolution. Since a certain surface potential can induce alignment of single CNTs on suitable charge patterns, we further demonstrate the creation of small CNT networks by nanoxerography.

The process for electrostatically guided deposition of CNTs and fullerenes is illustrated schematically in Figure 1. First, patterns of local surface charges are written into a thin electret layer by operating the atomic force microscope (AFM) in lithography mode (Figure 1A). The charge patterns are drawn by applying voltage pulses to the conductive AFM tip while the tip laterally moves over the grounded sample with tapping mode feedback turned on. Subsequently, the

* Corresponding author. E-mail: naujoks@nano.mavt.ethz.ch.

10.1021/nl0713373 CCC: $37.00
Published on Web 09/11/2007

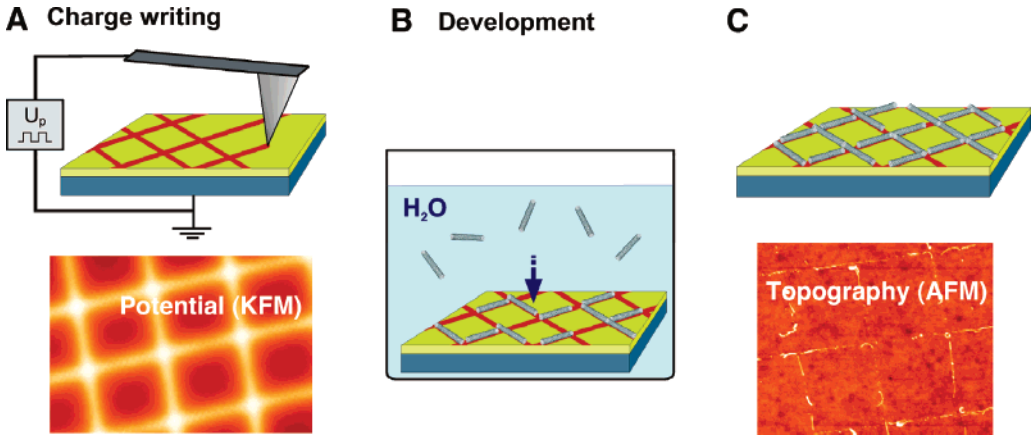

Figure 1. Nanoxerography process: (A) Charge patterns are written into an electret layer on a solid substrate by applying voltage pulses to a conductive AFM tip. Directly after the charge-writing process, the surface potential of the charge pattern is imaged in KFM. (B) To develop the charge patterns, the sample is immersed into an aqueous suspension containing the nanotubes or fullerenes to be deposited. (C) After the sample is rinsed in pure IPA and dried in air, the nanotubes or fullerenes are precisely attached to the predefined pattern.

charged template is immersed into a suspension containing surfactant-stabilized SWCNTs or C_{60} molecules, which are electrostatically attracted to the previously defined surface locations due to their surface charge (Figure 1B). Throughout all experiments, 100 nm thin poly(methyl methacrylate) (PMMA) layers on p-doped silicon wafers were used as electret layers. PMMA is an electret reported to have excellent charge-storing capabilities.[21] The layers were formed by spin coating a 5% solution of PMMA (M_w = 350 kDa) in toluene at 3500 rpm and subsequent baking on a hotplate at 180 °C for 3 min. Charge writing and imaging were performed using a Nanoscope Multimode AFM with a NanoScope IIIa controller (Digital Instruments Veeco Metrology Group, Santa Barbara, CA) and n-doped silicon tips with a resistivity of 0.01−0.025 Ω cm (Nanosensors, Neuchatel, Switzerland, type PPP-NCHR-W). Charge patterns were generated at tip-drawing velocities of 1−2 μm/s and a constant voltage pulse length of 2 ms at a pulse frequency of 100 Hz. The pulse amplitudes were set between 25 and 70 V, resulting in increases of the local surface potential in the range of ΔV = 0.2−2.5 V with reference to the background. Immediately after charge writing, the charged templates were characterized in situ by operating the AFM in Kelvin Force Microscopy (KFM) mode (Figure 1A).[22,23] The charge-patterned samples were then developed in freshly prepared suspensions for 30 s. Before being dried in an air stream, the samples were rinsed with isopropyl alcohol (IPA) to remove loosely bound CNTs or C_{60} molecules from the sample. The complete experimental course including charge writing, charge imaging, suspension preparation, sample development, and pattern imaging was accomplished in ambient under normal laboratory conditions.

Selectivity and precision achieved in nanoxerography of CNTs are illustrated in Figure 2, showing nanotubes attached to ten parallel lines that were charged to different surface potentials. A closer look reveals the width of attached nanotube stripes to correlate with the generated surface potentials. Figure 2A is a KFM image of the charge pattern, ten 20 μm long lines with 1.2 μm spacing, acquired immediately after charge writing, prior to sample development. Surface potentials between ΔV = 0.6 and 2.2 V were created by applying voltage pulses in the range of 25−70 V. SWCNTs (Cheap Tubes, Inc., Brattleboro, VT, nominal diameter 1−2 nm) were dispersed in UHQ water containing 5% weight per volume (w/v) of Synperonic NP10 (Sigma-Aldrich), a nonionic surfactant. A stable dispersion was achieved by ultrasonication for 10 min using an ultrasonic probe (Branson Digital Sonifier, model 450, Branson Ultrasonics) at a power level of 40 W, while keeping the dispersion in an ice-water bath. After sonication, the suspension was centrifuged at 75000*g* for 4 h, and the upper 90% of the supernatant was decanted for use. The resulting nanotube suspension had a typical mass concentration of 20−25 mg/L. The charged sample was developed in 1 mL of ice-cold nanotube suspension for 30 s. After the sample was rinsed and dried, the sample topography was imaged by AFM (Figure 2B).

The CNTs deposited exclusively onto positively charged patterns on the sample, leading to the assumption that the tubes carry a net negative surface charge and are attracted by means of Coulomb interaction. Since negatively charged patterns yielded no attachment of nanotubes (see Supporting Information), dielectric attraction can be excluded as the predominant driving force. The same phenomenon has been observed for carboxyl-functionalized CNTs solubilized in UHQ water, depositing selectively onto positively charged areas on PMMA.[20] The apparent negative surface charge on the nanotubes presumably arises from the surfactant, which attaches to the nanotubes with its hydrophobic part (a nine-carbon alkyl chain linked to a benzene ring), exposing the polar head group (a poly(ethylene oxide) (PEO) chain, ~10 units) to the aqueous solution. The benzene ring increases the binding of the surfactant to the nanotubes.[24] The PEO chain is nonionic, though it is highly polar and known to solubilize metal cations.[25] The tendency of PEO to complex metal cations is attributed to ion-dipole interactions, arising between the metal ion and the free electron pairs of the oxygen atoms of the PEO chain. The polarity of the C−O bonds leads to local dipoles in the PEO molecule: electrons are pulled toward the oxygen atoms, inducing negative partial

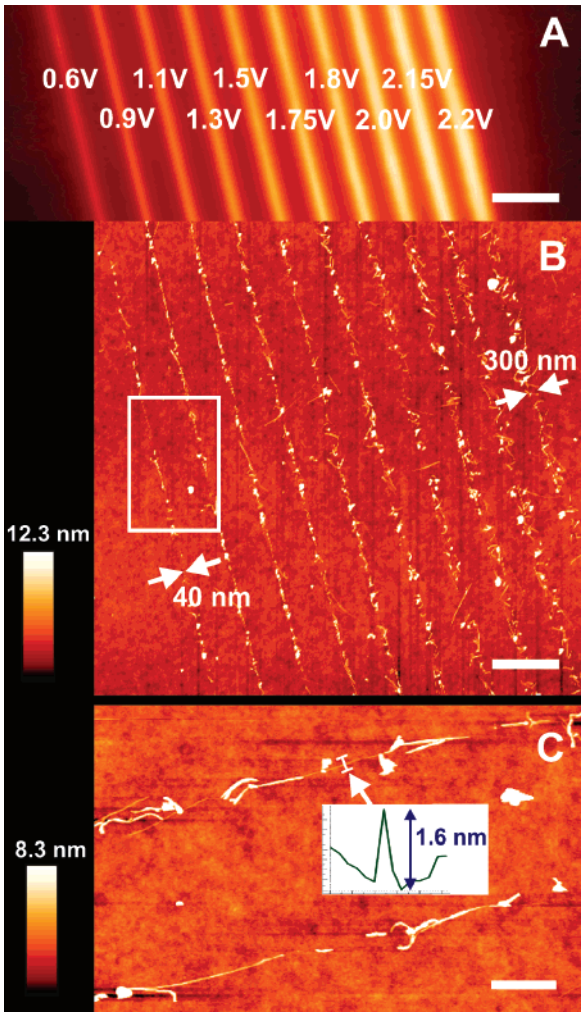

Figure 2. SWCNTs selectively deposited onto a pattern of ten parallel lines. (A) Surface potential of the charge pattern, imaged by KFM immediately after charge writing. The values indicate the peak surface potential of the line with reference to the background. Scale bar: 2 μm. (B) AFM topography image of the SWCNT pattern after development. The line widths of the SWCNT attachment range from 300 nm down to 40 nm, depending on the previously created surface potential. Scale bar: 2 μm. (C) Zoom into Figure 2B: at a surface potential of $\Delta V = 0.6-0.9$ V, the line patterns yield one single tube or one single bundle in width, well-aligned along the charged line. The profile plot indicates an individual SWCNT. Scale bar: 500 nm.

charges. These negative partial charges enable the PEO to form complexes with positive ions. In a polar environment, such as in water, the PEO molecules acquire a helical conformation, with the hydrophilic oxygen atoms facing outside of the molecular chain toward the solution and the hydrophobic ethylene groups embedded inside of the molecule.[26] We assume this mechanism is responsible for the attraction of the surfactant-stabilized CNTs to charge patterns of positive polarity on PMMA surfaces. The negative partial charges located at the oxygen atoms of the PEO chains face toward the water and can thus interact with positive charges written into the PMMA surface, leading to a selective attraction of nanotubes.

With reduction of the amount of deposited charge, the stripes covered by nanotubes get thinner, down to straight lines of single tubes at surface potentials of around $\Delta V = 0.5$ V (Figure 2C). The broader stripes are homogeneously covered by CNTs and show a well-defined line width over their entire length. Furthermore, the selectivity of this nanoxerography process is so high that virtually no tubes attach to the background around the pattern. The high selectivity presumably arises from the PMMA background acquiring a negative zeta-potential when immersed into aqueous solutions,[27,28] such as the surfactant-based suspension used here. The negative zeta-potential repels the negatively charged nanotubes from the PMMA surface. To explore the potential of nanoxerography in more detail, we investigated the deposition of C_{60} molecules. Chemically, buckminsterfullerenes are closely related to carbon nanotubes but may reproduce the charge patterns with higher accuracy due to their smaller size and round shape.

To this end, C_{60} aggregates were deposited from aqueous suspension onto a charge pattern similar to the one used for CNT deposition (Figure 3A). A stable suspension was prepared by adding 10% w/v of the nonionic surfactant Triton X-100 (poly(ethylene glycol) *tert*-octylphenyl ether), which is nearly identical to Synperonic NP10 (poly(ethylene glycol) nonylphenyl ether); the two surfactants only differ by the length of the alkyl chain attached to the benzene group. Again, the C_{60} aggregates only deposited onto positively charged patterns, implying that Coulomb forces constitute the dominant mechanism guiding the aggregates onto the charged patterns. The line pattern further documents the feasibility of controlling the line width of attached material by varying the surface potential. The line width of the C_{60} patterns decreases with decreasing surface potential and can be reduced down to the formation of a single string of small aggregates at a surface potential of $\Delta V = 0.5$ V (Figure 3D). Detailed inspection of Figure 3B reveals that only eight of ten lines are clearly covered. No attachment of C_{60} molecules occurs on lines with surfaces potentials below $\Delta V = 0.3$ V, suggesting the existence of a threshold surface potential for particle attraction. As observed for the CNTs, the fullerenes deposit with high yield and specificity, leaving the PMMA background nearly clean.

The highly similar deposition behavior of C_{60} molecules and SWCNTs strengthens our hypothesis that the negative charge guiding the particles toward the positively charged patterns is generated at the surfactant-water interface and does not require surface charges on the particles themselves (see section on deposition of CNTs). We further assume that the deposition process of CNTs and fullerenes is influenced by the concentration and ratio of positive and negative ions in the suspension. When a nonionic surfactant is used, the aqueous suspension contains only few additional ions, resulting in a sufficiently thick electric double layer above the substrate to allow for efficient electrostatic attraction of SWCNTs or C_{60} molecules from the liquid phase. Furthermore, since no additional negative ions are present in the solution, the positive surface charges in the PMMA are not neutralized by smaller highly mobile ions before the nanotubes deposit on the pattern. As for the SWCNT patterns, the C_{60} line patterns show clearly defined borders, and the

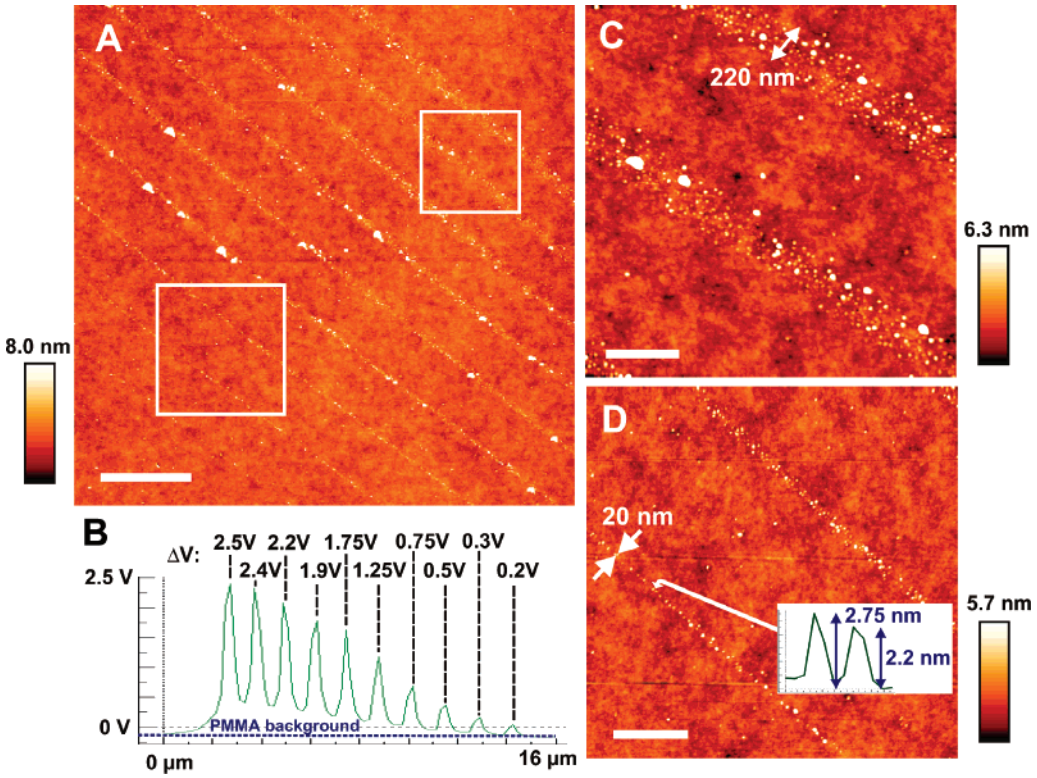

Figure 3. C_{60}-fullerenes selectively deposited onto a pattern of ten parallel lines. (A) AFM topography image of the C_{60} pattern after development. Eight of ten lines are clearly covered by C_{60} clusters. Scale bar: 2 μm. (B) Profile plot of the surface potential immediately after charge writing. (C) Zoom into Figure 3A: the C_{60} attachment is dominated by 2−5 nm sized clusters as well as C_{60} monomers, with sporadic clusters larger than 5 nm. Scale bar: 400 nm. (D) Zoom into Figure 3A: at a surface potential of $\Delta V = 0.5$ V, the fullerenes attach as a string of single clusters. The profile plot illustrates two small clusters of 2.75 and 2.2 nm diameter. Scale bar: 600 nm.

line width varies monotonously with the surface potential. On comparison of SWCNT and C_{60} patterns, specific surface potentials appear to correspond to qualitatively equal line width. For example, peak potentials of $\Delta V = 2.0-2.5$ V measured after charge writing yield 200−300 nm wide lines of attached particles after development in both cases. Peak potentials of $\Delta V = 0.5$ V even lead to lines of roughly one particle diameter in width, corresponding to less than 20 nm line width. As evidenced in parts C and D of Figure 3, the fullerene attachment is dominated by 2−5 nm sized clusters as well as C_{60} monomers that are homogeneously distributed over the full line width.

The suspension of C_{60} in UHQ water and Triton X-100 was achieved by a similar procedure as described by Beeby et al.[29] In brief, 0.5 mg of C_{60} (Sigma-Aldrich) was dissolved as a molecular solution in 2 mL of toluene. A concentrate of C_{60} in surfactant was prepared by mixing the C_{60} toluene solution with 0.5 g of pure Triton X-100 (Sigma-Aldrich) and subsequent evaporation of the toluene. The resulting transparent orange-colored suspension was further diluted with 5 mL of UHQ water under mild sonication. The final suspension contained 0.5 mg of C_{60} in 5 mL of UHQ water with 10% w/v of Triton X-100 surfactant. The development was performed as described previously.

Encouraged by the fact that SWCNTs individually align along charge lines of approximately $\Delta V = 0.5$ V surface potential (Figure 2), we explored the creation of small nanotube networks. The attachment of CNTs to two different geometries, a straight network and a sine-shaped pattern, is illustrated in Figure 4.

The suspension for the rectangular network shown in Figure 4A was equally prepared as the suspension used in Figure 2. The nanotube deposition was achieved in one development step. The rectangular network is predominantly composed of lines of one single SWCNT or one SWCNT bundle in width. At some nodes, nanotubes or nanotube bundles are deposited onto each other, forming a right angle crossing (Figure 4A(a)). At other locations, nanotubes or nanotube bundles appear to form interconnections along straight lines (b). Apparently, the negative charge on the nanotubes is too weak to completely prevent nanotube deposition onto already deposited nanotubes. Nevertheless, to build an intact complete SWCNT network, further improvement would be needed to overcome the number of interrupts (c). Depositing the perpendicular tube lines in two sequential process steps may be a possibility to further improve pattern reproduction. The suspension used for the development of the sinusoidal pattern shown in Figure 4B was prepared by dispersing 1 mg of raw nanotube material in a 10 mL solution of 5% w/v Synperonic NP10 surfactant. After sonication, the ice-cooled suspension was used immediately, without further centrifugation. Hence, the fraction of long nanotubes is higher in these suspensions, though they also contain more bundles and entangled nanotubes than the centrifuged ones. As the sinusoidal pattern emphasizes, the nanoxerography method is capable of attaching SWCNTs

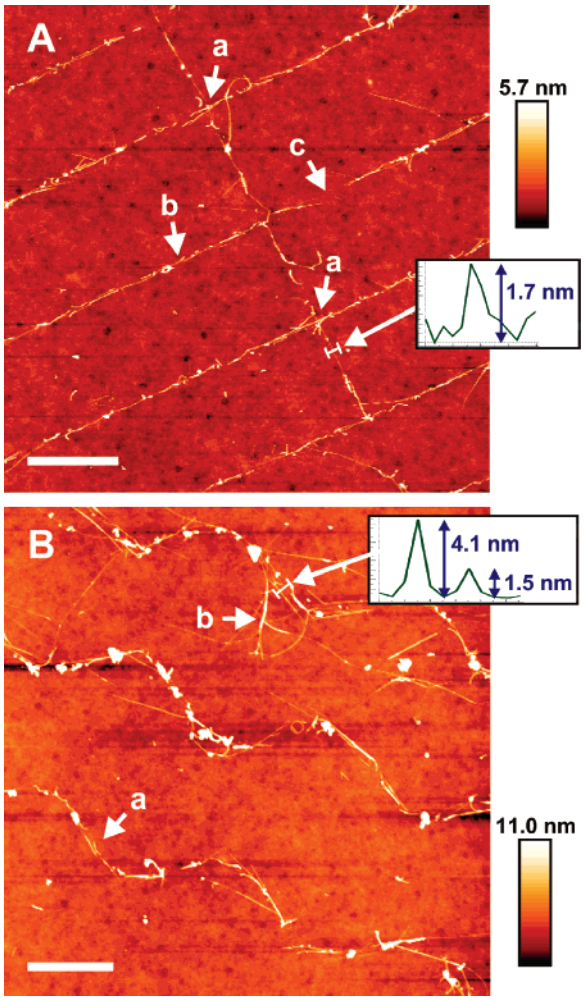

Figure 4. Small CNT networks assembled from individual SWCNT and SWCNT bundles. (A) The straight perpendicular nanotube network shows locations of crossing nanotubes (a), nanotube interconnections along straight lines (b), but also interrupts (c). The insert illustrates the profile across a well-aligned SWCNT. Scale bar: 1.5 μm. (B) Sine-shaped pattern featuring regions of CNTs well aligned to the pattern (a), as well as regions where nanotubes shear out of the intended directions (b). The insert is a profile plot across a SWCNT bundle of 4.1 nm diameter and an individual SWCNT. Scale bar: 1.5 μm.

to curved geometries to a certain extent. Bending and buckling of carbon nanotubes present a topic explored in a number of contributions. Zou et al. showed the assembly of SWCNTs bent into rings of 200 nm in diameter and demonstrated that bending of the nanotubes depends on the interaction strength between tube and substrate.[26] The sine pattern in Figure 4B features regions where the charge pattern is clearly reproduced (a), as well as regions where nanotubes shear out of the intended direction of alignment (b). While single CNTs may be easily aligned on the pattern via the electrostatic forces from the charge patterns, a substantially higher force might be required to overcome the stiffness of nanotube bundles.

In summary, we have shown how single-walled carbon nanotubes, as well as fullerene molecules, can be precisely deposited and aligned onto electret surfaces, using patterns of local surface charges. Particle attachment is achieved by immersing the charged sample into an aqueous suspension containing CNTs or C_{60} molecules, stably dispersed using a nonionic surfactant. We have demonstrated that the surface potential of the written charges constitutes a crucial parameter for controlling the particle attachment. Surface potential and line width of attached particles show a strong correlation. With this method, a pattern resolution in the range of one particle diameter can be achieved using small surface potentials in the range of $\Delta V = 0.5$ V.

During development of the sample in the aqueous suspension, the surface potential of the charge patterns drops substantially. Even though, the particles strongly attach to the substrate as evidenced by their stability against vigorous rinsing with IPA or water. We conclude that whereas particle attraction is guided by electrostatic Coulomb forces, final attachment of particles is dominated by van der Waals forces. Hence, the surfactant can be washed away by generously rinsing the sample, without removing the nanotubes from the patterns (see Supporting Information).

Preparation of suitable CNT suspensions still represents a challenging task,[27] since they often contain CNTs of a wide range of lengths, as well as CNT bundles and nanoparticle clusters. Similarly, C_{60} aggregates with diameters ranging from 2 to 10 nm are found in the fullerene suspensions. Optimizing the suspensions toward single CNTs of uniform length and monodisperse C_{60} will further improve deposition results achievable with nanoxerography. Our process is a further step toward simpler methods for creating CNT arrays and networks with high accuracy and flexibility in geometry, as well as toward the precise deposition of single fullerenes.

Supporting Information Available: Descriptions and images of deposition behavior of CNTs on positive and negative charge patterns and removal of surfactant by rinsing. This material is available free of charge via the Internet at http://pubs.acs.org.

References

(1) Bachtold, A.; Hadley, P.; Nakanishi, T.; Dekker, C. *Science* **2001**, *294*, 1317.
(2) Yuzvinsky, T. D.; Fennimore, A. M.; Kis, A.; Zettl, A. *Nanotechnology* **2006**, *17*, 434.
(3) Rueckes, T.; Kim, K.; Joselevich, E.; Tseng, G. Y.; Cheung, C.; Lieber, C. M. *Science* **2000**, *289*, 94.
(4) Kong, J.; Franklin, N. R.; Zhou, C.; Chapline, M. G.; Peng, S.; Cho, K.; Dai, H. *Science* **2000**, *287*, 622.
(5) Stampfer, C.; Helbling, T.; Obergfell, D.; Schöberle, B.; Tripp, M. K.; Jungen, A.; Roth, S.; Bright, V. M.; Hierold, C. *Nano Lett.* **2006**, *6*, 233.
(6) Fan, S.; Chapline, M. G.; Franklin, N. R.; Tombler, T. W.; Cassell, A. M.; Dai, H. *Science* **1999**, *283*, 512.
(7) Yamamoto, K.; Akita, S.; Nakayama, Y. *J. Phys. D: Appl. Phys.* **1998**, *31*, L34.
(8) Krupke, R.; Hennrich, F.; von Löhneysen, H.; Kappes, M. M. *Science* **2003**, *301*, 344.
(9) Xin, H.; Woolley, A. T. *Nano Lett.* **2004**, *4*, 1481.
(10) Im, J.; Lee, M.; Myung, S.; Huang, L.; Rao, S. G.; Lee, D. J.; Koh, J.; Hong, S. *Nanotechnology* **2006**, *17*, 3569.
(11) Wang, L.; Liu, B.; Liu, D.; Yao, M.; Hou, Y.; Yu, S.; Cui, T.; Li, D.; Zou, G.; Iwasiewicz, A.; Sundqvist, B. *Adv. Mater.* **2006**, *18*, 1883.
(12) Backer, S. A.; Suez, I.; Fresco, Z. M.; Ronaldi, M.; Fréchet, J. M. J. *Langmuir* **2007**, *23*, 2297.
(13) Barry, C. R.; Gu, J.; Jacobs, H. O. *Nano Lett.* **2005**, *5*, 2078.
(14) Jacobs, H. O.; Whitesides, G. M. *Science* **2001**, *291*, 1763.

(15) Mesquida, P.; Stemmer, A. *Adv. Mater.* **2001**, *13*, 1395.
(16) Mesquida, P.; Stemmer, A. *Microelectron. Eng.* **2002**, *61*, 671.
(17) Naujoks, N.; Stemmer, A. *J. Nanosci. Nanotechnol.* **2006**, *6*, 2445.
(18) Mesquida, P.; Ammann, D. L.; MacPhee, C. E.; McKendry, R. A. *Adv. Mater.* **2005**, *17*, 893.
(19) Cao, T.; Xu, Q.; Winkleman, A.; Whitesides, G. M. *Small* **2005**, *1*, 1191.
(20) Seemann, L.; Stemmer, A.; Naujoks, N. *Microelectron. Eng.* **2007**, *84*, 1423.
(21) Sessler, G. M. *Electrets*; Springer, Berlin, 1987.
(22) Jacobs, H. O.; Knapp, H. F.; Muller, S.; Stemmer, A. *Ultramicroscopy* **1997**, *69*, 39.
(23) Nonnenmacher, M.; O'Boyle, M. P.; Wickramasinghe, H. K. *Appl. Phys. Lett.* **1991**, *58*, 2921.
(24) Islam, M. F.; Rojas, E.; Bergey, D. M.; Johnson, A. T.; Yodh, A. G. *Nano Lett.* **2003**, *2*, 269.
(25) Cowie, J. M. G.; Cree, S. H. *Annu. Rev. Phys. Chem.* **2003**, *40*, 85.
(26) Sui, X.; Shao, C.; Liu, Y. *Polymer* **2007**, *48*, 1459.
(27) Fa, K.; Paruchuri, V. K.; Brown, S. C.; Moudgil, B. M.; Miller, J. D. *Phys. Chem. Chem. Phys.* **2005**, *7*, 678.
(28) Beattie, J. K. *Lab Chip* **2006**, *6*, 1409.
(29) Beeby, A.; Eastoe, J.; Heenan, R. K. *J. Chem. Soc., Chem. Commun.* **1994**, *10*, 173.
(30) Zou, S.; Maspoch, D.; Wang, Y.; Mirkin, C. A.; Schatz, G. C. *Nano Lett.* **2007**, *7*, 276.
(31) Hennrich, F.; Krupke, R.; Arnold, K.; Rojas Stütz, J. A.; Lebedkin, S.; Koch, T.; Schimmel, T.; Kappes, M. M. *J. Phys. Chem.* **2007**, *111*, 1932.

NL0713373